International Journal of Engineering and Emerging Scientific Discovery
ISSN: 2536-7250 (Print): 2536-7269 (Online)
Volume 7, Number 3, September 2022
http://www.casirmediapublishing.com

Design and CFD Analysis of a Fixed-Wing Unmanned Aerial Vehicle for Surveillance Purpose

Taye Stephen Mogaji[1*], Adegoke Ezekiel Fadiji[2], Babatunde David Oladipupo[1]
[1]Department of Mechanical Engineering, School of Engineering and Engineering Technology, Federal University of Technology, Akure, PMB 104, Ondo State, Nigeria
[2]Department of Electrical Electronic Engineering, Bamidele Olumilua University of Education, Science and Technology, Ikere Ekiti, Ekiti State, Nigeria
Email: mogajits@gmail.com; Corresponding Author: Taye Stephen Mogaji[1*]

ABSTRACT
This article is based on the design and CFD analysis of a long-range fixed wing unmanned aerial vehicle (UAV) suitable for wide area surveillance. Taking a systems approach, the components of the UAV were designed and applied with Burke's framework. The conceptual drawing of the proposed fixed wing UAV was done using Solidworks computer aided design CAD application software. The designed UAV has a span of 1.5m and fuselage length of 1.135m. Computational Fluid Dynamics (CFD) Analysis was ran on the fixed wing UAV to evaluate its performance. The CFD result revealed that the upper surface of the wing experiences a higher velocity than the bottom surface as expected. It is also found that the aircraft is stable statically and dynamically during flight period of simulation test. Other simulation results carried out showed that the design is considered safe and fit for fabrication. The fixed wing UAV when fabricated can be used for surveillance purpose suitable for civilian and military applications.
Keywords: fixed wing UAV, CFD, conceptual design, simulation

INTRODUCTION
Air transportation had long been in use by the civilians for commercial purposes and by the military; these aircraft had great importance in our lives today and could still fit into more places in our lives. One of the most used area is for commercial transportation, these had connected the world as humans of different races can easily reach each other and work together, share knowledge, receive training and tourism (Fischer, 2011; Leibold, 2020). The military had also use aircraft for war, transportation of aids to war zones, delivery of troops for reinforcement in some cases, surveillance, reconnaissance and many other use cases like mapping and research (Ananthasayanam et al., 2005). Aircrafts are generally any craft crafted for the purpose of moving in the air. Thus, an aircraft does not necessarily need to carry men, a kite is thus an aircraft since it is crafted to achieve flight.

Aircraft are of different types, there are aircraft which achieved their flight by buoyancy, these are made to be lighter than air by use of large balloons filled with light gases which could be hot air, hydrogen, helium; these are referred to as Lighter than air aircrafts (Mercado, 2017).

A specially crafted device called the airfoil generate lift when air flows past it and was used to achieve lift heavier than air aircrafts. This airfoil can be used in two distinct ways; it could be attached to the aircraft frame as fixed wings and made to run through the air till it develops enough lift to fly and are called fixed wings aircraft. The airfoil could also be rotated on a vertical mast as rotating wings, as it rotates and flows past air, it generates lift to achieve its fight and are thus called rotary winged aircraft or rotorcraft (Raymer, 2019). The fixed wing aircraft must reach a certain speed before takeoff, thus, most fixed wing aircrafts takeoff horizontally, such aircrafts undergo horizontal takeoff and landing (HTOL). Rotorcrafts on the other hand achieve lift through its revolution, thus, it has to reach a minimum revolution per minute before takeoff and does not require to run before take. Therefore, rotary wing aircrafts are capable of vertical takeoff and landing (VTOL) (Garrison, 2020).As pointed out in the studies of (Boon et al., 2017; Friedmann, 2001), Fixed wing generally has higher cruising speed as compared to rotorcraft, thus, they are transition aircrafts capable of vertical takeoff and landing, it will thus, transit or switch to from VTOL to normal fixed wings, thereby achieving high cruising speeds in other words, transition aircrafts takeoff vertically like rotary wings and fly horizontally like fixed wings.

Fixed wings have higher cruising speed, longer range while rotorcrafts can do vertical takeoff landing, capable of hovering, denote that fixed wings are more suitable for longer range missions or high-speed applications and altitude (fixed wing altitude depends on the propulsion system in use, design and some other factors). According to Camillo (2013), Rotorcrafts are more suited for rescue mission due to its ability to hover in the air, it also finds application in relatively low speed as compared to fixed wings. Both fixed wing and rotary wings may be suited for similar applications, but different requirement may make them both suited and they may be adapted with design for specialized application. Therefore, with the view of averting persistent insecurity challenges in the society and achieving

International Journal of Engineering and Emerging Scientific Discovery
ISSN: 2536-7250 (Print): 2536-7269 (Online)
Volume 7, Number 3, September 2022
http://www.casirmediapublishing.com

expected effective rescue mission appropriate for civilian and military applications, design and CFD analysis of a long-range fixed wing unmanned aerial vehicle (UAV) suitable for wide area surveillance is carried out in this research.

METHODOLOGY

Aircraft design phases involving two major stages known as the acquisition stage and the utilization stage shown in Figure 1 as described extensively by (Sadraey, 2020) is adopted in this study.

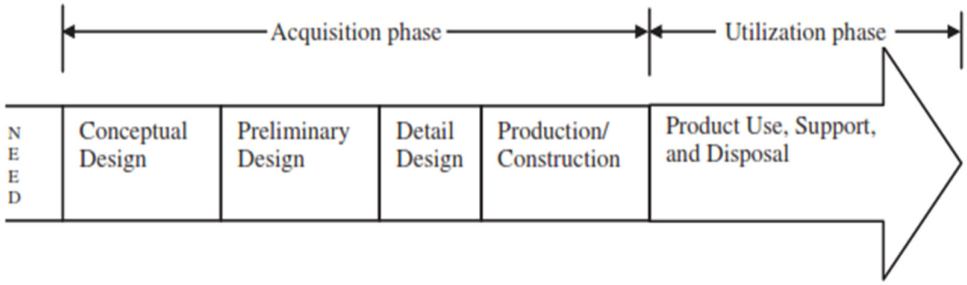

Figure 1: Aircraft design phases (Sadraey, 2020)

Component Breakdown

The major components that the aircraft requires in order to satisfy the design requirements are highlighted as (i) Wing: necessary for lift generation. The mid-wing configuration was selected because it offers the easiest means to connect with the fuselage from a structural point of view as well as the advantage of little interference drag (Sadraey, 2020). The UAV would be a monoplane (one wing) and fixed sweep, (ii) Tail for control and stability during flight. The conventional tail was selected because of its simplicity for manufacture, it offers the least structural weight and control mix. (iii) The fuselage a simple hollow box with an aerodynamic shape that helps in supporting the landing gear. It would be unpressurized and would have top, bottom and side hatches to allow access to internal electronics, (vi) Structural configuration: to hold components together in flight and on ground. A lightweight and locally obtainable material would be employed for the structural components like light wood and carbon fibre, (v) Propulsion system: to generate thrust. The propulsion system would be battery-powered electric motors and propeller. The propulsion would be tractor rather than pusher to ensure that the propulsion system weight stays close to the centre of gravity.

The batteries would be Lithium-based batteries based on their high energy density, (vi) Landing gear: to support the aircraft weight on ground. The landing gear would be tricycle in order to avoid the complexities in take-off associated with tail dragger (Hull, 2007). The landing gear would be fixed with the aircraft and (vii) Communication and control electronics: to control and capture images and communicate with ground receiver. It would have a camera payload to capture video feed and transmit over the internet to a ground control station.

Design Analysis.

Determination of the wing planform area, wingspan and chord distributions

The wing planform area, wingspan and chord distributions of the aircraft system were determined using Eqns. (1 – 4) given as follows:

$$\lambda = \frac{C_t}{C_r} \quad (1)$$

$$AR = \frac{b^2}{S} \quad (1)$$

$$\therefore S = wing\ area = \frac{b^2}{AR} \quad (2)$$

$$S = b \times \bar{C} = \frac{weight}{wing\ loading} \quad (3)$$

Where: λ is wing sweep angle, C_t is wing tip chord, C_r is wing root chord, AR is the wing aspect ratio, b is the wing span, S is the wing surface area, $\bar{C}$ is the mean aerodynamic chord of the wing

Bending Moment of the Wing and Horizontal Tail

An approximation of the lift distribution was obtained using the Lifting Line Theory implemented in XFLR5 and the bending moment over the wing surface was calculated as shown in Figure 2.

International Journal of Engineering and Emerging Scientific Discovery
ISSN: 2536-7250 (Print): 2536-7269 (Online)
Volume 7, Number 3, September 2022
http://www.casirmediapublishing.com

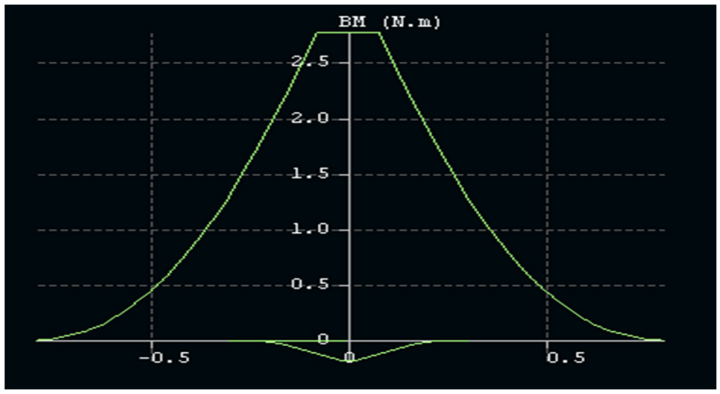

Figure 2: Bending moment distribution along the span of the wing and horizontal tail

From the plot in Figure 2, the maximum bending moment is 2.76N.m. The budge in the bottom of the figure above shows the bending moment for the horizontal tail with a minimum bending moment of -0.2N.m. With this information, carbon fibre rods were selected to act as wing spars with a central wing box made of balsa wood due to its high strength-to-weight ratio. The carbon fibre rods have a diameter of 2mm and a length of 500mm which was the standard size of the material in the market.

Stability and Control of the Aircraft

An aircraft has three moment about any fixed point linked to its center of gravity given as follow:

Pitching

$$C_m = \frac{M}{qSc} \tag{5}$$

Yawing

$$C_n = \frac{N}{qSb} \tag{6}$$

Rolling

$$C_L = \frac{L}{qSb} \tag{7}$$

Moderate changes in angle of attack will have negligible or no influence on the aircraft yaw and roll, the same is true for roll and yaw as they also have negligible or no influence on pitching moment. For this reason, stability control analysis is usually divided into longitudinal analysis

concerned (pitch analysis) and lateral analysis (roll and yaw stability analysis).The moment about the center of gravity which the craft stability in flight is determined considering Eqns. (8-12) as follow:

$$M_{cg} = L(X_{cg} - X_{acw}) + M_w + M_{w_{\delta f}}\delta f + M_{fus} - L_h(X_{ach} - X_{cg}) - TZ_t + F_p(X_{cg} - X_p) \quad (8)$$

Where: L is lift on the wing, L_h is lift on the horizontal tail, T is the thrust on the propeller, F_p is vertical force due to the propeller, M_{cg} is the total moment on the center of gravity, M_w is wing moment, M_{fus} is the fuselage moment, $M_{w_{\delta f}}$ is the wing moment derivative with respect to flap deflection, X_{cg} is the location of the centre of gravity, X_{acw} is the wing aerodynamic center, X_{ach} is the tail aerodynamic center, X_p is the propeller location, Z_t is the height of the propeller from the center of gravity. The equation of moment about the centre of gravity of the aircraft can also be expressed in terms of dimensionless coefficients as follows:

$$C_{m_{cg}} = C_L(\bar{X}_{cg} - \bar{X}_{acw}) + C_{m_w} + C_{m_{w\delta f}}\delta f + C_{m_{fus}} - \eta_h \frac{S_h}{S_w} C_{L_h}(\bar{X}_{ach} - \bar{X}_{cg}) - \frac{T}{qS_w}\bar{Z}_t + \frac{F_p}{qS_w}(\bar{X}_{cg} - \bar{X}_p) \quad (9)$$

The term η_h in Eq. (9) is defined as the system tail dynamic pressure ratio given as

$$\eta_h = \frac{q_h}{q} \quad (10)$$

Static trim condition of the system is achieved when the $C_{m_{cg}}$ is zero. To achieve static stability, changes in angle of attack must result in moments in the opposite sense of the change, resulting in restoring moments (a negative value of C_{m_α}; thus, to achieve this, the derivative of the pitching moment with respect to angle of attack must be negative and the expression is given as follows:

$$C_{m_\alpha} = C_{L_\alpha}(\bar{X}_{cg} - \bar{X}_{acw}) + C_{m_{\alpha fus}} - \eta_h \frac{S_h}{S_w} C_{L_{\alpha h}} \frac{\partial \alpha_h}{\partial \alpha}(\bar{X}_{ach} - \bar{X}_{cg}) + \frac{F_{p_\alpha}}{qS_w}\frac{\partial \alpha_p}{\partial \alpha}(\bar{X}_{cg} - \bar{X}_p) \quad (11)$$

The aircraft will experience neutral stability when Eq. (11) equates to zero. The location of the $C_{m_{cg}}$ at which this occurs is known as the neutral point

International Journal of Engineering and Emerging Scientific Discovery
ISSN: 2536-7250 (Print): 2536-7269 (Online)
Volume 7, Number 3, September 2022
http://www.casirmediapublishing.com

X_{np} which is determined by equating the Eq. (11) to zero. At this point, the pitching moment does not change as the angle of attack changes. This is mathematically expressed as:

$$\bar{X}_{np} = \frac{C_{L_\alpha}\bar{X}_{acw} - C_{m_{\alpha fus}} + \eta_h \frac{S_h}{S_w} C_{L_\alpha} \frac{\partial \alpha_h}{\partial \alpha} \bar{X}_{ach} + \frac{F_{p_\alpha}}{qS_w} \frac{\partial \alpha_p}{\partial \alpha} \bar{X}_p}{C_{L_\alpha} + \eta_h \frac{S_h}{S_w} C_{L_{\alpha h}} \frac{\partial \alpha_p}{\partial \alpha}} \quad (12)$$

$\bar{X}_{np}$ is the most-aft centre of gravity location before the aircraft becomes unstable. Another important term is static margin (SM), which is determined as the difference between neutral point and the centre of gravity.

$$SM = \bar{X}_{np} - \bar{X}_{cg} \quad (13)$$

By substituting the parameters of the tail into Eq. (13), the neutral point, moment slope of the system is designed for.

Determination of the Aircraft system Taper Ratio

The taper ratio is the ratio of the tip chord to the root chord given as follows:

$$. \lambda = \frac{c_t}{c_r} = \frac{tip\ chord}{root\ chord} \quad (14)$$

Based on Eq. (14), the taper ratio for the wing, tail and their respective flapped ratio are determined.

The Fixed wing UAV Design Drawings

The conceptual drawing of the proposed fixed wing UAV based on the design calculation was done using Solidworks computer aided design CAD application software because of the provision for features such as; 3D solid modelling and simulation, large and complex assembly design, automatic drawing view creation and update, advanced surface design and flattening, direct model editing and CAD import/export to mention but a few. The conceptual design of the proposed fixed wing UAV in this study is presented in Figure 3 while the orthographic and isometric views of the designed UAV is shown in Figure 4. Display in Figure 5 is the generated tail airfoils of the designed fixed wing UAV

,

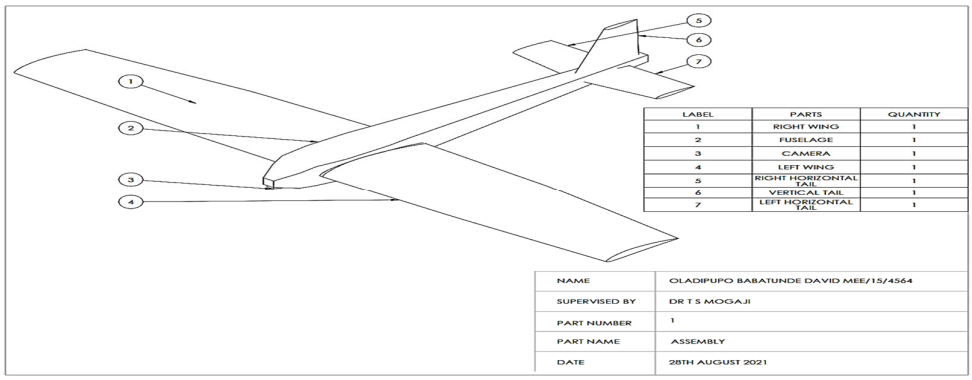

Figure 3: Conceptual designed of the fixed wing UAV

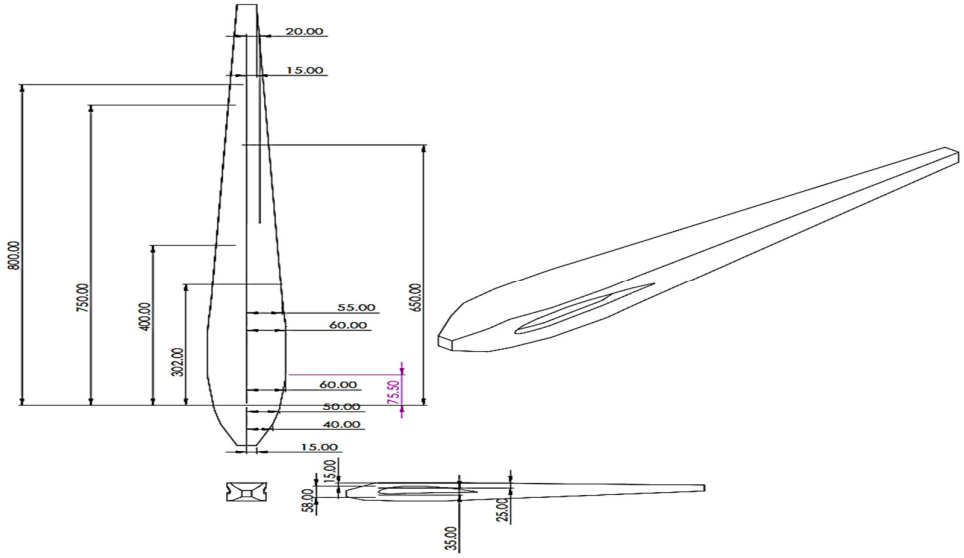

Figure 4: Orthographic and isometric views of the fuselage

International Journal of Engineering and Emerging Scientific Discovery
ISSN: 2536-7250 (Print): 2536-7269 (Online)
Volume 7, Number 3, September 2022
http://www.casirmediapublishing.com

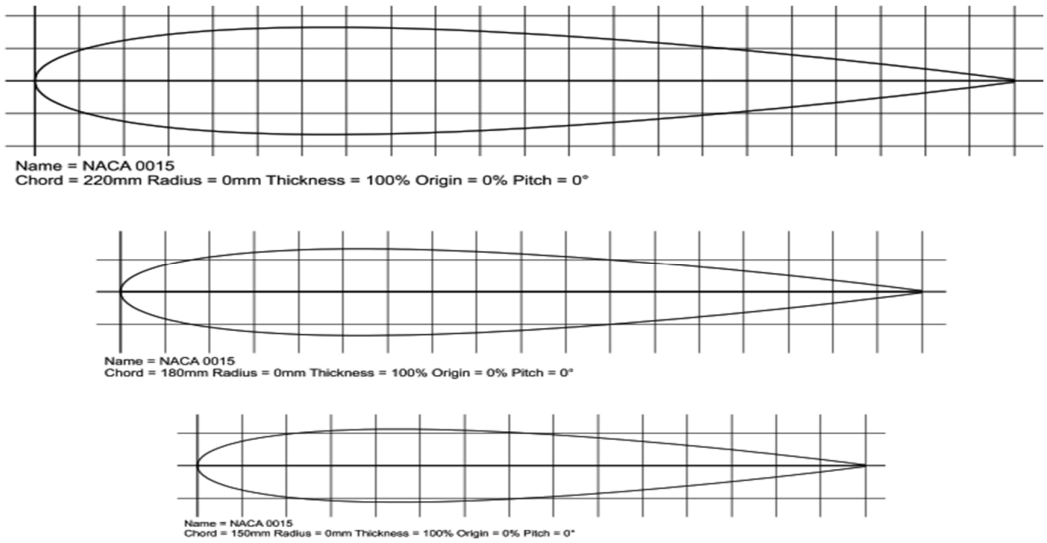

Figure 5: Generated tail airfoils of the designed fixed wing UAV

RESULTS AND DISCUSSION

Simulation result of the fixed wing UAV

Computational Fluid Dynamics (CFD) Analysis was ran on the fixed wing UAV considering: calculated take-off velocity of 12.13m/s, selected cruise velocity as 15m/s, calculated landing velocity of 9.1m/s, calculated flight time of 12.9 minutes and range of the aircraft as 11.6 km. The cruise flight of the UAV was setup as a fluid dynamics simulation in Solidworks environment. The velocity was set to 15 m/s which is the cruise velocity. Furthermore, air model which includes 40% humidity was setup to account for the weather humidity. Shown in Figure 6 is the global fluid mesh of the air around the designed UAV in this work.

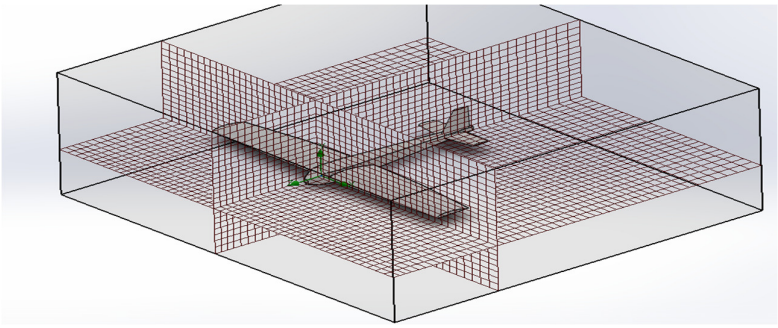

Figure 6: Global fluid mesh of the air around the designed fixed wing UAV.

Upon the completion of the simulation which took 6.5 hours, the pressure field around the wings at quarter-chord location is as shown in Figure 7. The simulation predicts a lift following a close-to-elliptic shape as expected.

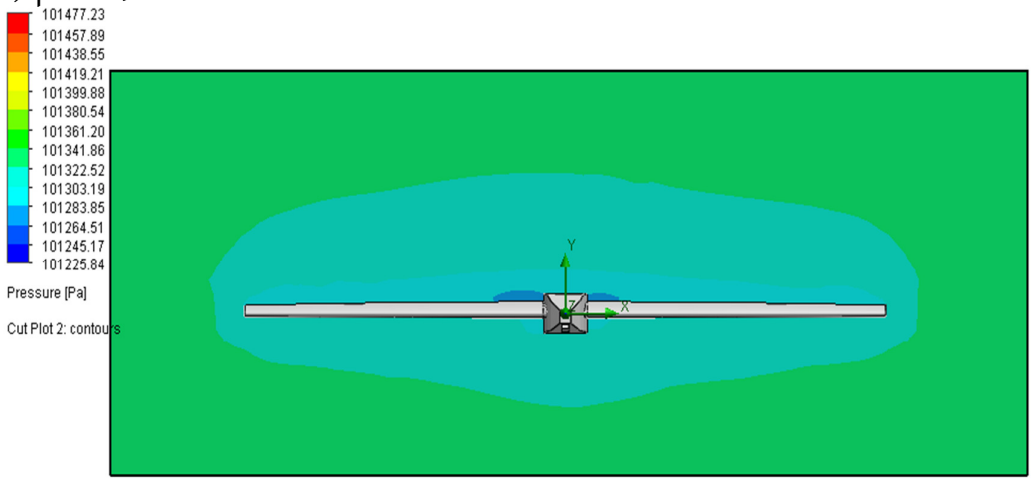

Figure 7: Pressure field around the designed fixed wing UAV

The pressure experienced by each surface of the UAV is shown in Figure 8 revealing stagnation point on the leading edge of the designed UAV wing. It is also observed that considering a severe source of interference drag and flow separation the fuselage has no adverse pressure points as depicted in Figure 8.

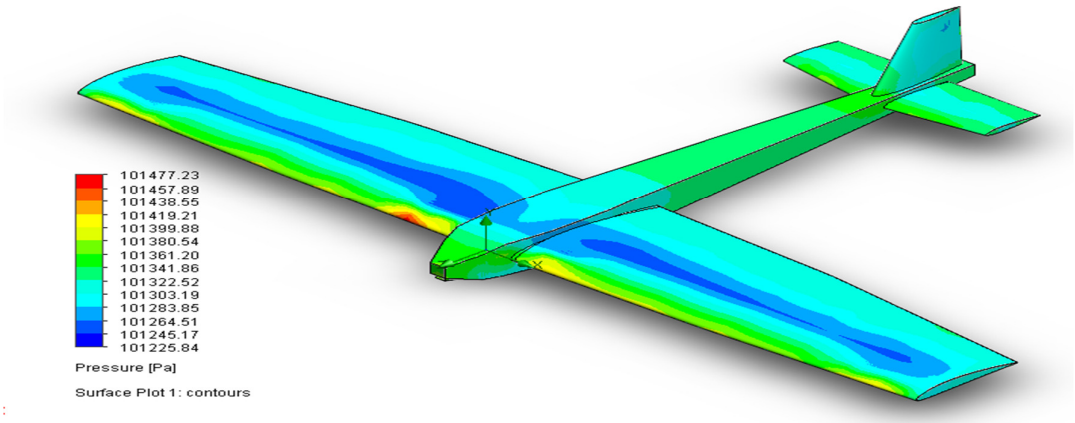

Figure 8: Surface plot showing pressure distribution over the UAV

Presented in Figure 9 is the flow trajectories of the air over the left wing of the designed UAV in this work. The CFD result reveals the pinching

International Journal of Engineering and Emerging Scientific Discovery
ISSN: 2536-7250 (Print): 2536-7269 (Online)
Volume 7, Number 3, September 2022
http://www.casirmediapublishing.com

of the airflow over the top surface of the wing and spread of the air flow over the bottom surface of the aircraft. This behavior aids the upper surface of the wing experiences a higher velocity than the bottom surface as expected.

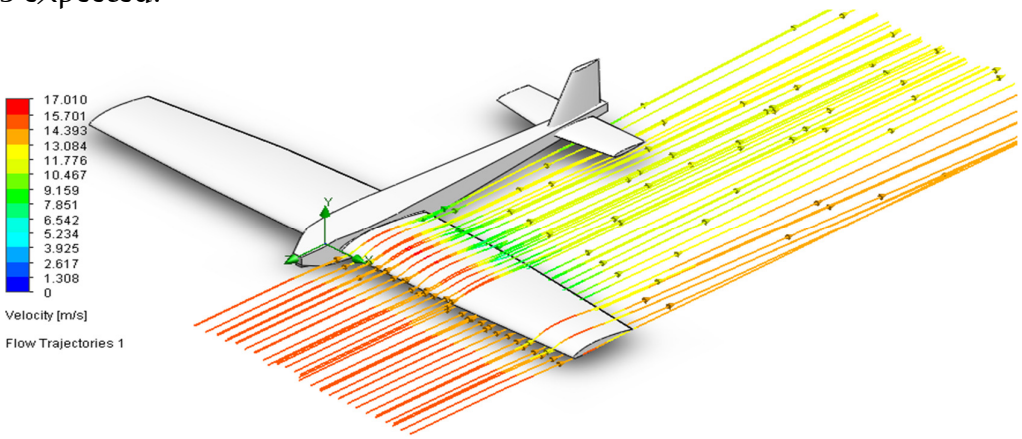

Figure 9: Flow trajectories over left wing of UAV

Simulation of the Designed UAV

The observed simulation behavior of the designed UAV in connection to the lateral component of the aircraft after receiving an upward gust of 1 m/s is shown in Figure 10a. The result from the figure revealed that the aircraft was able to stabilize laterally in 90 seconds. This behavior indicates that the aircraft is stable statically and dynamically. Moreso, the simulated result of the designed UAV presented in Figure 10b also revealed that the aircraft after take-off returned back to trim condition in a certain amount of allowable time as the aircraft damps quickly to a very comparable low value in 50 seconds. Presented in Figure 11 is the flow trajectories along the fuselage of the UAV at 15m/s considering the lift distribution on the aircraft using 1° angle of attack. From this Figure, the wing of the designed UAV is seen to have an upward lift distribution which is elliptical due to the double tapered wing. The lift distribution on the horizontal tail is also visible from the image and increase towards the fuselage. The total lift on the aircraft is the summation of the lift on the horizontal tail and the wing. The aerodynamic center is behind the wing and very close to the center of gravity, the red curved arrow indicates an aerodynamically nose down moment which balance the nose up moment of the weight of the aircraft, thus, allowing the aircraft to trim

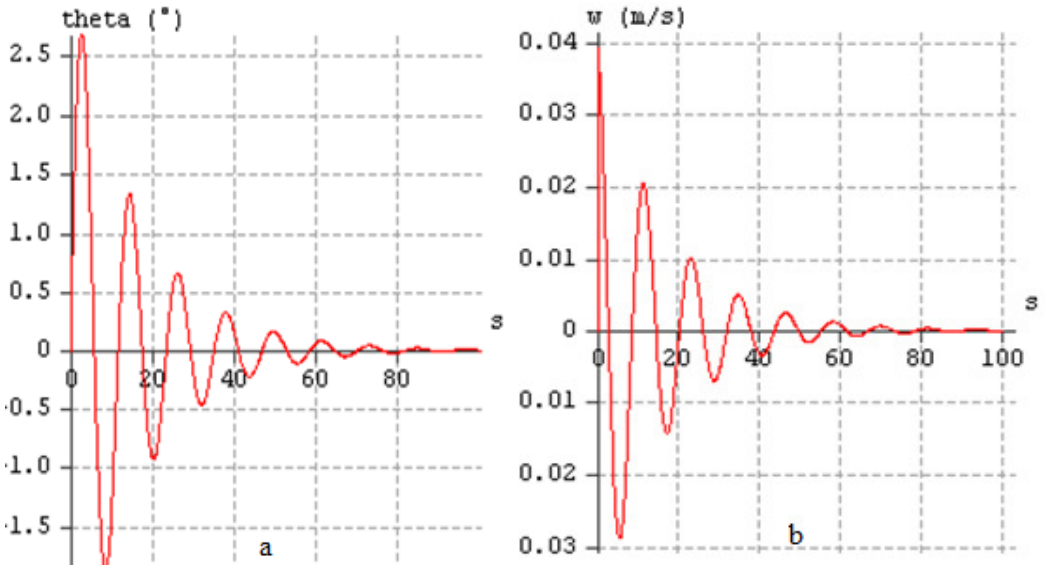

Figure 10: Variation of aircraft angle and nose-up pitching speed at 1m/s sudden upward gust.

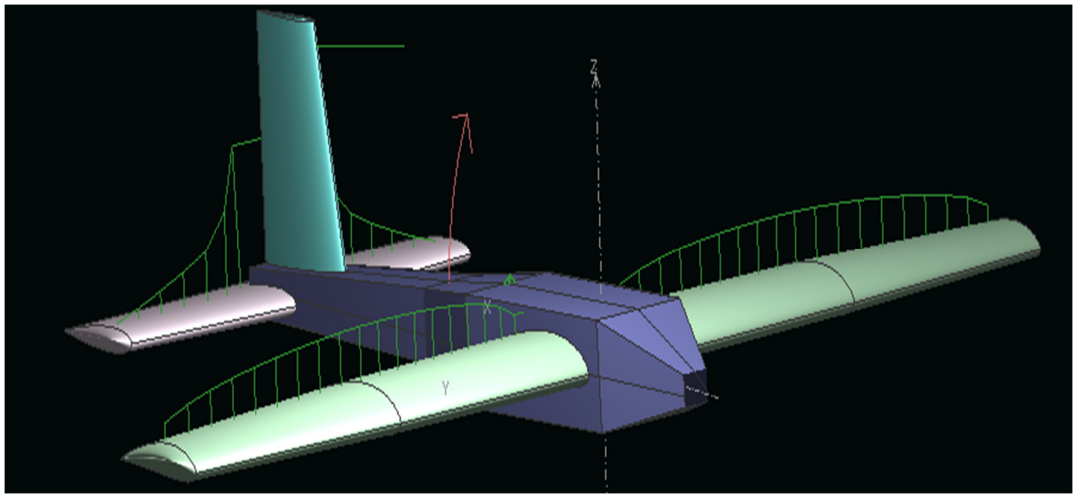

Figure 11: Lift distribution along wing and horizontal stabilizer at 1° angle of attack and 15m/s forward velocity

CONCLUSION

A fixed wing unmanned aerial vehicle (UAV) was designed and simulated in this study. The designed UAV has a span of 1.5m and fuselage length of 1.135m. To accomplish a longer range, the control signals and video stream are designed to be transmitted through the internet connection indicating that the designed UAV in this work is not

limited by the use of Wireless controllers. Amazon Virtual private Cloud was also used to ensure secure communication and control of the aircraft system. The considered telemetry streaming of video of the designed UAV to the ground based station proves as another functionality which is very useful for surveillance as the aircraft will be able to provide live and instantaneous coverage based on the mission requirement. The pressure experienced by each surface of the designed fixed wing UAV based on CFD result in this study revealed that the fuselage has no adverse pressure points considering a severe source of interference drag and flow separation. Additionally, the upper surface of the wing experiences a higher velocity than the bottom surface as expected during the pinching of the airflow over the top surface of the wing and spread of the air flow over the bottom surface of the aircraft. Thus, the designed fixed wing UAV is suitable for civilian and military applications.

ACKNOWLEDGEMENT

The authors would like to acknowledge the assistance of Department of Mechanical Engineering, Federal University of Technology Akure in supplying relevant information used in the present study.

CONFLICT INTEREST

The authors declared that there is no conflict interest on the article.

REFERENCES

Ananthasayanam, M. R., Ibrahim, K. and Muralidharan, M. R. (2005). Historical evolution of the military fighter airplanes around the twentieth century. *43rd AIAA Aerospace Sciences Meeting and Exhibit - Meeting Papers, March*, 6609–6619. https://doi.org/10.2514/6.2005-326

Boon, M. A., Drijfhout, A. P. and Tesfamichael, S. (2017). Comparison of a fixed-wing and multi-rotor UAV for environmental mapping applications: A case study. *International Archives of the Photogrammetry, Remote Sensing and Spatial Information Sciences - ISPRS Archives*, *42*(2W6), 47–54. https://doi.org/10.5194/isprs-archives-XLII-2-W6-47-2017

Camillo, E. dl. (2013). *A brief history of the evolution of transportation over time*. 1–5. https://www.centrostudisubalpino.it/lang1/files/Brief-

hystory-of-transport.pdf

Fischer, B. B. (2011). Spy dust and ghost surveillance: How the KGB spooked the CIA and hid Aldrich Ames in plain sight. *International Journal of Intelligence and CounterIntelligence*, *24*(2), 268–306. https://doi.org/10.1080/08850607.2011.548205

Garrison, W. L. (2020). Historical Transportation Development. *Transportation Engineering and Planning*, *I*. *General Aviation Aircraft Design : Applied Methods*. (n.d.).

Leibold, J. (2020). Surveillance in China's Xinjiang Region: Ethnic Sorting, Coercion, and Inducement. *Journal of Contemporary China*, *29*(121), 46–60. https://doi.org/10.1080/10670564.2019.1621529

Mercado, M. (2017). *The Rise and Fall of Lighter-Than-Air Aircraft , 1783*. *17*(1).

Raymer, D. (2019). Aircraft Design: A Conceptual Approach, Sixth Edition and RDSwin Student SET. In *Aircraft Design: A Conceptual Approach, Sixth Edition and RDSwin Student SET*. https://doi.org/10.2514/4.105746

Sadraey, M. (2020). *Aircraft design: a systems engineering approach*.